DESIGN AND PERFORMANCE OF WAVEGUIDE E-PLANE HTSC INSERT FILTERS

Liang Han, Yiyuan Chen and Yunyi Wang
State Key Laboratory of Millimeter Waves
Southeast University, Nanjing 210018, P.R. China

Qiheng Cheng, Senzhu Yang and Peiheng Wu
Department of Information Physics
Nanjing University, Nanjing 210008, P.R. China

ABSTRACT — A design theory is described for waveguide E-plane inductive strip filters that takes the high order mode interaction and finite thickness of metal with dielectric substrate underneath into account. An X-band bandpass filter is fabricated with High-Tc Superconducting (HTSC) material. The measured results of the HTSC bandpass filter are presented and compared with the CAD predicted filter performances.

I. INTRODUCTION

Recent developments and technology breakthroughs in the microwave and millimeter-wave will lead to rapid development of HTSC passive and active components. And on the other hand, microwave superconductivity will play a more and more important part in the design and development of microwave and mm- wave components, because of low insertion losses and negligible frequency dispersion. In addition, HTSC technology will offer significant reductions in weight, size and power consumption. Taking filter as example, the HTSC material can significantly improve the passband insertion loss and skirt selectivity because of the high Qs of the HTSC lines [1]-[2]. Recently, the superconducting waveguide filter has been reported [3], whose waveguide housing is made of HTSC and inductive strips are in form of silver-plated metal.

The conventional design of finline filter [4]-[5] for HTSC application is limited by the area of HTSC thin films in the X- band. The main idea of this paper is to use superconducting material, instead of metal, in the design of inductive strip insert filters (Fig.1). A design method is introduced for this purpose, and the HTSC films serve as perfect conductors.

The method is verified by measurement. The measured frequency response of the HTSC bandpass filter that has been designed and operated at X-band shows good agreement between theory and measured results. The minimum insertion loss of the filter is $0.25dB$ at the temperature of $71.5K$.

This project is supported by National Superconductor Research Center

II. THEORY

Considering one section of waveguide E-plane inductive strip insert (Fig.2a), because of the symmetry, the scattering parameters of the structure can be found easily from the symmetric network theory,

$$S_{11} = \frac{1}{2}(S^e_{11} + S^o_{11}) \tag{1a}$$

$$S_{21} = \frac{1}{2}(S^e_{11} - S^o_{11}) \tag{1b}$$

if the even and odd mode reflection coefficients S^e_{11} and S^o_{11} are found respectively. For even mode the geometrical symmetric plane in Fig.1 is supposed to be a magnetic wall and for the odd mode an electrical wall.

For each subregion (Fig.2b), the components of electromagnetic fields are assumed to be a sum of suitable eigenmodes,

$$E^{(1)}_y = \sum_{m=1}^{p}(V^{(1)+}_m + V^{(1)-}_m)e^{(1)}_{y,m} \tag{2a}$$

$$H^{(1)}_z = \sum_{m=1}^{p}(V^{(1)+}_m - V^{(1)-}_m)h^{(1)}_{z,m} \tag{2b}$$

IF2

and

$$E_y^v = \sum_{n=1}^{q} V_n^v e_{y,n}^v \begin{cases} \cos(k_{z,n}^v W), & \text{even mode} \\ j\sin(k_{z,n}^v W), & \text{odd mode} \end{cases} \quad v=(2),(3) \quad (3a)$$

$$H_z^v = \sum_{n=1}^{q} V_n^v h_{z,n}^v \begin{cases} j\sin(k_{z,n}^v W), & \text{even mode} \\ \cos(k_{z,n}^v W), & \text{odd mode} \end{cases} \quad v=(2),(3) \quad (3b)$$

where

$$e_y, n^v = -j\omega\mu \sin(k_x, n^v x)$$

$$h_x, n^v = jk_z, n^v \sin(k_x, n^v x) \qquad v=(1),(2)$$

$$e_y, n^{(3)} = j\omega\mu[\sin k_x, n^{(3)'}(a-x)U' + \frac{\sin k_x, n^{(3)'} a_2}{\sin k_x, n^{(3)''} d} \sin k_x, n^{(3)''}(x-a_1-t)U'']$$

$$h_x, n^{(3)} = jk_z, n^{(3)}[\sin k_x, n^{(3)'}(a-x)U' + \frac{\sin k_x, n^{(3)'} a_2}{\sin k_x, n^{(3)''} d} \sin k_x, n^{(3)''}(x-a_1-t)U'']$$

$$U' = \begin{cases} 1, & a_1+t < x < a_1+t+d \\ 0, & otherwise \end{cases}$$

$$U'' = \begin{cases} 1, & a_1+t+d < x < a \\ 0, & otherwise. \end{cases}$$

k_z^v and k_x^v are the wave numbers in Z and X directions, and mode votlages $V^{\pm}$ are the still unknown eigenmode amplitudes of the forward and backward waves.

By matching the field components at corresponding interfaces,

$$E_y^{(1)} = \begin{cases} E_y^{(2)}, & (x,y) \in F^{(2)}; \\ E_y^{(3)}, & (x,y) \in F^{(3)}; \\ 0, & (x,y) \in F^t. \end{cases} \quad (4a)$$

$$H_z^{(1)} = \begin{cases} H_z^{(2)}, & (x,y) \in F^{(2)}; \\ H_z^{(3)}, & (x,y) \in F^{(3)}. \end{cases} \quad (4b)$$

the mode votages in Eqs. (2) and (3) can be related to each other after taking inner product with appropriate orthogonal functions,

$$[K_1]([V^{(1)^+}] + [V^{(1)^-}]) = [T_1][V^{(2)}] + [T_2][V^{(3)}] \quad (5a)$$

$$[P_1]([V^{(1)^+}] - [V^{(1)^-}]) = [K_2][V^{(2)}] \quad (5b)$$

$$[P_2]([V^{(1)^+}] - [V^{(1)^-}]) = [K_3][V^{(3)}] \quad (5c)$$

This yields the one-port scattering matrix at the step discontinuity $Z=0$,

$$[V^{(1)^-}] = [S_{11}^e][V^{(1)^+}], \quad \text{for even mode} \quad (6a)$$

and

$$[V^{(1)^-}] = [S_{11}^o][V^{(1)^+}], \quad \text{for odd mode} \quad (6b)$$

respectively. The coefficient matrices and $S_{11}^{o,e}$ are explained in the Appendix. The scattering matrix of the inductive strip can be determined from Eq.(1). And several finite length inserted strips are cascaded with waveguide separations to form a filter circuit.

III. DESIGN

Based on the theory above, a FORTRAN optimization program of bandpass filter is developed. The parameters $l_1 - l_n$ and $W_1 - W_n$ that are defined in Fig.4 are optimized for the given insertion losses in the passband, the attenuations in the stopband, the number of resonators, the thickness of dielectric substrate and of metal or HTSC thin film coating.

For an E-plane metal insert filter with two resonators, the design data are obtained by letting $\varepsilon_r = 1$ and $a_1 = d + a_2$ in this program. Fig.3 shows the insertion loss curves of the filter calculated by our method, whose sizes are taken from [6]. The results of [6] are also shown in the same figure for comparison. As expected, the given results of [6] agree well with our results.

The configuration of two-resonator HTSC bandpass filter is shown in Fig.4. The HTSC films (YBCO) are coated on one side of $LaAlO_3$ substrate. The thickness of HTSC films and substrates are chosen to be $t = 2000\AA$ and $d = 0.5mm$, respectively. The substrates ($\varepsilon_r = 21$) with HTSC films are then inserted in a metal waveguide. The HTSC films below the critical temperature are considered as perfect conductors and the waveguides between the substrates as resonators of the filter.

IV. FILTER PERFORMANCE

Fig.5 shows the calculated and measured insertion loss ($1/|S_{21}|$) and return loss ($1/|S_{11}|$) in decibels as a function of frequency for a two-resonator X-band E-plane HTSC filter. The calculated minimum insertion loss in the pass band is $0.01dB$, and the measured value is about $0.25dB$ at the temperature of $71.5K$. The measured insertion losses are attributed to the ones of metal housing, substrates and HTSC films.

V. CONCLUSION

An X-band bandpass filter made of superconducting film insert is firstly developed with an improved design method of waveguide E-plane inductive strip insert filter, and experimental results at liquid nitrogen temperature are presented with the minimum insertion loss of $0.25dB$. It shows the promising application of superconducting material to microwave E-plane filters. The results indicate that the design method for microwave passive components with perfect conductors has the sufficient accuracy to HTSC.

APPENDIX

In Eq.(5), the elements of each matrix are

$$[V^{(v)}] = [V_1^{(v)}, V_2^{(v)}, ...]^T, \qquad v = (1),(2),(3)$$

$$K_1(i,i) = A^{(2)} \int_0^a e_{y,i}^{(1)} \times (h_{x,i}^{(1)})^* dx$$

$$K_2(j,j) = A^{(3)} \int_0^{a_1} h_{x,j}^{(2)} \times (e_{y,j}^{(2)})^* dx$$

$$K_3(j,j) = \int_{a_1+t}^{a} h_{x,j}^{(3)} \times (e_{y,j}^{(3)})^* dx$$

$$P_1(i,j) = \int_0^{a_1} h_{x,i}^{(1)} \times (e_{y,j}^{(2)})^* dx$$

$$P_2(i,j) = \int_{a_1+t}^{a} h_{x,i}^{(1)} \times (e_{y,j}^{(3)})^* dx$$

$$T_1(i,j) = B^{(2)} \int_0^{a_1} e_{y,j}^{(2)} \times (h_{x,i}^{(2)})^* dx$$

$$T_2(i,j) = B^{(3)} \int_{a_1+t}^{a} e_{y,j}^{(3)} \times (h_{x,i}^{(2)})^* dx$$

where

$$A^v = \begin{cases} j\sin(k_z^v W), & \textit{even mode} \\ \cos(k_z^v W), & \textit{odd mode} \end{cases} \qquad v = (2),(3)$$

$$B^v = \begin{cases} \cos(k_z^v W), & \textit{even mode} \\ j\sin(k_z^v W), & \textit{odd mode} \end{cases} \qquad v = (2),(3)$$

and in Eq.(6),

$$[S_{11}] = ([K_1] + [U_1] + [U_2])^{-1}([U_1] + [U_2] - [K_1])$$

$$[U_1] = [T_1][K_2]^{-1}[P_1]$$

$$[U_2] = [T_2][K_3]^{-1}[P_2]$$

REFERENCES

[1] A.R. Jha, "Applications of High-Temperature Superconductors in Millimeter-Wave Components and Circuits", The 3rd APMC Proceedings, Tokyo, 1990, pp.607-612.

[2] P.A. Macdonald, D. Rensch, J.Y. Josefowicz, F. Williams and W. Hoefer, "Characterization of Microstrip Discontinuities on $LaAlO_3$", 1991 IEEE MTT-S Digest, 1991, pp.1341-1344.

[3] R.R. Mansour and A. Zybura, "Superconducting Millimeter Wave E-Plane Filters", IEEE Trans. on MTT, Vol. 39, No.9, Sept. 1991, pp.1488-1492

[4] F. Arndt, J. Bornemann, D. Grauerholz and R. Vahldieck, "Theory and Design of Low-Insertion Loss Fin-Line Filters", IEEE Trans., on MTT, Vol.MTT-30, No.2, Feb., 1982, pp.155-162.

[5] Y. Shih, T. Itoh and L.Q. Bui, "Computer Aided Design of Millimeter Wave E-plane Filters", IEEE Trans. on MTT, Vol.MTT-31, No.2, Feb. 1983, pp.135-141.

[6] R. Vahldieck, J. Bornemann, F. Arndt and D. Grauerholz, "Optimized Waveguide E-plane Metal Insert Filters for Millimeter Wave Applications", IEEE Trans. on MTT, Vol.MTT- 31, No.1, 1983, pp.65-69.

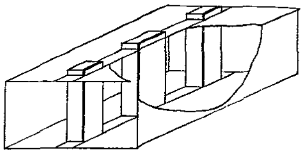

Fig. 1 Inductive strip insert filter supported by dielectrics

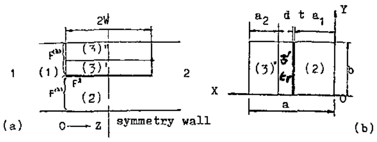

Fig. 2 Transition waveguide to inductive strip and cross section with common interface

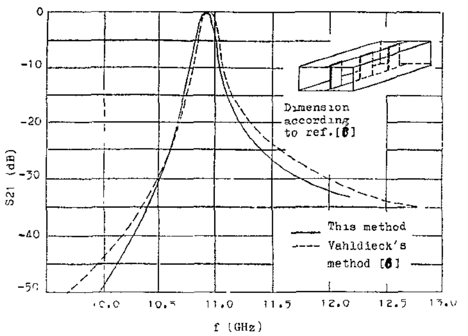

Fig. 3 Comparsion of insertion losses of X-band metal insert filter calculated by our method and ref. [6]

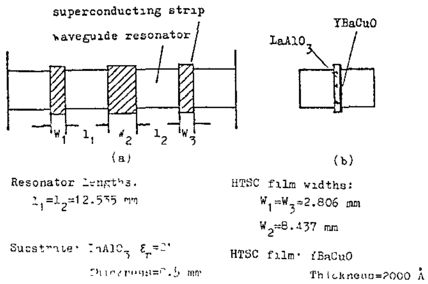

Fig. 4 Configuration of two-resonator HTSC band pass filter

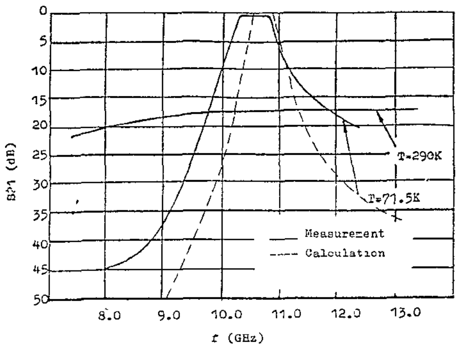

(a) Insertion loss characteristics

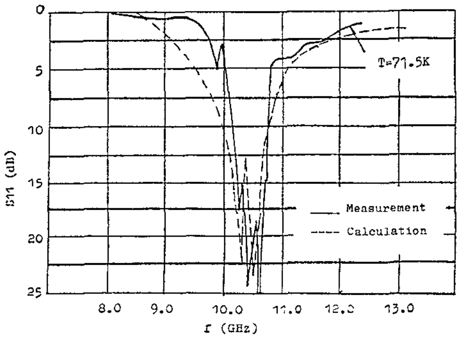

(b) Return loss characteristics

Fig. 5 Frequency responses for the filter in Fig. 4.